

WAMS-BASED HIERARCHICAL ACTIVE POWER DIFFERENTIAL SIGNAL ALGORITHM FOR BACKUP PROTECTION OF A FACTS COMPENSATED TRANSMISSION NETWORK

Sreelekha VENUGOPAL¹ , Prince ASOK¹ , Sabha Raj ARYA² 

¹Department of Electrical Engineering, Rajiv Gandhi Institute of Technology, APJ Abdul Kalam Technological University, Alathara Rd, 695016 Kerala, India

²Department of Electrical Engineering, Sardar Vallabhbhai National Institute of Technology, Ichchhanath, Surat, 395007 Gujrat, India

svlekha@gmail.com, prince@rit.ac.in, sabharaj94@gmail.com

DOI: 10.15598/aece.v20i4.4512

Article history: Received Mar 22, 2022; Revised Jul 20, 2022; Accepted Jul 27, 2022; Published Dec 31, 2022.
This is an open access article under the BY-CC license.

Abstract. *This paper proposes a hierarchical active power differential signal-based generalized backup protection algorithm using Wide Area Measurement System (WAMS) data for Flexible AC Transmission System (FACTS)-compensated transmission networks. The proposed algorithm can be used for backup protection of transmission systems with any shunt and series-type FACTS devices. The increased number of FACT compensators affects the reliable operation of primary and backup protection of the transmission lines. Both shunt and series compensated lines cause malfunctioning of existing backup protection schemes. The proposed algorithm utilizes the sequence components of bus voltages and active power differential signals of lines to identify the faulty line. The algorithm is validated on a modified 9-bus system under MATLAB/SIMULINK platform. It is observed that the algorithm is suitable for identifying a faulty line in transmission systems containing both uncompensated and compensated lines with series or shunt-type FACTS controllers. This algorithm has the advantage that it uses a generalized backup protection logic and can be used for the accurate identification of a faulty line irrespective of the type of compensation devices.*

Keywords

Backup protection, FACTS devices, faulty line identification, PMU, Power differential protection, Superimposed power component, WAMS.

1. Introduction

As the power demand goes on increasing with industrial developments and commercial activities, the power transmission system is being modified. Due to environmental reasons and right-of-way restrictions, construction and the addition of a completely new transmission path may be difficult and impossible. The efficient utilization of the existing power transmission system by including Flexible AC Transmission System (FACTS) devices is a preferred alternative for the problem, which increases the power transmission capability of lines with improved stability margins and control of power [1]. FACTS compensators alter the magnitude and phase angle of the apparent line impedance and line current, as seen by the protection devices. The existing relays are designed for uncompensated lines and their settings do not consider the presence of compensating devices and the variation of line impedance or current values due to their compensating actions. Hence the incorporation of FACTS devices in transmission systems causes the malfunctioning of distance relays,

introduces problems in the operation of the existing protection system, and affects the reliable operation of primary and backup protection [2] and [3]. Both shunt and series compensated lines cause problems in existing protection schemes. In the present scenario, it is necessary to develop a generalized protection scheme that can take care of the protection issues caused by the compensated lines also.

The development of a secured remote backup protection scheme using wide-area measurement system-based data for the present-day transmission system is very essential for secure operation [4]. Several transmission line protection algorithms have been developed using different techniques for relaying applications. Traveling wave-based and transient component-based fault detection schemes need higher sampling rates for the capture of details in the signals [6], [7], [8] and [9]. Differential current-based techniques [10], [11], [12], [13] and [14] and impedance-based estimation techniques [15], [16] and [17] are also well described in the literature. But these techniques cannot be used as generalized algorithms in the presence of compensating devices.

Various techniques are proposed by the researchers for the backup protection of uncompensated lines using Wide Area Measurement System (WAMS)-based data. By estimating and analyzing the distribution of sequence components of fault voltage the faulty bus can be identified [17]. Positive sequence voltage magnitude and absolute angle difference of positive sequence current angle are effective in identifying the faulty bus and the faulty line in a system with uncompensated lines [18]. In [19], the faulty region is identified using differential currents, and the faulty line is determined by a fault correlation factor calculated using the steady-state components of voltage and current. An active power differential-based logic is effective for the primary and backup protection schemes of uncompensated lines utilizing Phasor Measurement Unit (PMU) data [20]. A synchrophasor-based state estimator can be used for the backup protection of transmission lines [21]. But these algorithms do not consider the effects of compensating devices.

FACTS devices help to improve the steady-state and transient performance of the system. But the presence of these controllers poses many problems in the operation of the protective relays due to the fast control actions, impedance changes of the line, voltage and current injected from the control devices, and the transients produced by the control actions. When the device is included in the fault loop, it affects the apparent impedance seen by the distance relay causing its maloperation. The type of FACTS device has also its effect on the apparent impedance seen by the relay and trip boundary. A backup

protection scheme for series compensated lines based on the magnitudes and angles of positive and negative sequence voltages and currents is found more effective to avoid the malfunctioning of the relay in the presence of series compensation [22]. The modified impedance method for series compensated lines requires the measurement or estimation of voltage across the compensating device [23]. Spectral energy calculations based differential protection scheme using the Discrete Wavelet Transform (DWT) technique are proposed in [24] for SVC compensated lines. Fault detection in Fixed Series Capacitor (FSC) compensated lines can be achieved using differential admittance [25]. Sequence and superimposed components-based logic can be used for fault detection in the presence of Unified Power Flow Controller (UPFC) compensated lines [26] and [27]. Impedance-based techniques and differential apparent power-based techniques are also developed to avoid the malfunctioning of relays in the presence of UPFC [28], [29] and [30]. But these algorithms developed for compensated systems have considered only one type of device and its effects at a time and cannot be generalized. This work attempts to develop a generalized backup protection scheme based on WAMS-based data which utilizes the power differential value to identify the faulty line. It utilizes sequence components of bus voltages to identify the buses near a fault and the hierarchical magnitudes of differential active power signals to identify the faulty line. The proposed algorithm successfully detects the symmetrical and unsymmetrical fault conditions in a transmission system and the faulty line as well. The algorithm is validated in a modified WSCC 9 bus system incorporating FACTS devices and gives a reliable performance during different fault conditions and different line loading conditions. This paper is organized as follows. In Sec. 2, description of the power differential concept is given. The proposed algorithm is explained in detail in Sec. 3. Simulation results are discussed in Sec. 4. The conclusion is presented in Sec. 5.

2. Active Power Differential of a Transmission Line

A power difference exists between the two terminals of a transmission line, due to the losses in the transmission line, which increase with the load. Figure 1 shows π model of a transmission line. \bar{V}_x, \bar{V}_y are the voltages \bar{I}_x, \bar{I}_y are the line currents at bus X and bus Y . Z_L, Z_{xg} and Z_{yg} are the parameters of the π equivalent model of the line. The sources E_s and E_r with source impedances Z_s and Z_r are connected to the transmission line at X and Y . The apparent power at terminal X and Y be \bar{S}_x and \bar{S}_y respectively. The differential

active power Pd_{xy} is the real part of the differential apparent power $(\bar{S}_x - \bar{S}_y)$.

$$Pd_{xy} = \Re(\bar{S}_x - \bar{S}_y), \tag{1}$$

$$\bar{S}_x = \bar{V}_x \times \bar{I}_x, \tag{2}$$

$$\bar{S}_y = \bar{V}_y \times \bar{I}_y. \tag{3}$$

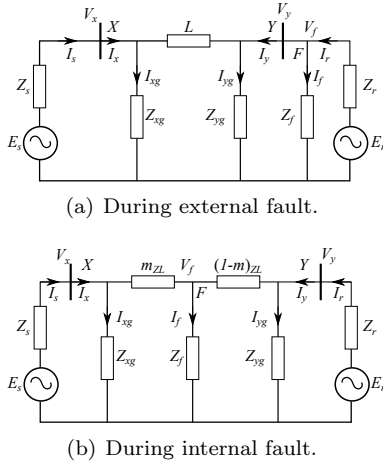


Fig. 1: Equivalent circuit of line.

The expression for this differential power is different when there is a fault within the line and when there is a fault outside.

Case 1. Differential power for an external fault.

In Fig. 1(a) an external fault occurs at point F outside the line.

The differential apparent power:

$$\bar{S}_1 - \bar{S}_2 = \left(\frac{\bar{V}_x^2 - \bar{V}_y^2}{z_g} \right) + \left(\frac{\bar{V}_x^2 - \bar{V}_y^2}{z_L} \right). \tag{4}$$

Case 2. Differential power for internal faults.

For an internal fault at F as shown in Fig. 1(b), the expression for line terminal currents can be written as follows. m is the distance of fault point from bus X expressed as a fraction of the distance between bus X and Y.

The differential apparent power:

$$\bar{S}_x - \bar{S}_y = \frac{\bar{V}_x^2 - \bar{V}_y^2}{z_g} + \frac{\bar{V}_x^2}{mz_Lz_f} - \frac{\bar{V}_y^2}{(1-m)z_Lz_f}. \tag{5}$$

Comparing Eq. (4) and Eq. (5), it can be observed that the differential apparent power value is considerably large in the case of internal faults. During faults, the real part of the differential power is large because of the high value of fault currents. Hence it can be used to identify a fault in a line. In the case of FACTS

compensated lines, this differential active power during normal operation of the line includes the normal losses of the device in its operating range. FACTS devices can inject or absorb reactive power into the system, but cannot produce active power on their own unless they are connected to a source that can supply active power. During abnormal conditions, these devices get bypassed by their protection circuits. So, the active power differential can be effectively used for the detection of a fault in the compensated lines also.

3. Hierarchical Active Power Differential Relaying Signal Based Backup Protection Algorithm

A WAMS-based differential power protection scheme for transmission systems containing a FACTS compensated line is proposed in this section. As shown in Fig. 2, the information from different substations of the protected area is collected at the PDC. The proposed algorithm utilizes the sequence components derived from bus voltages, taking advantage of the fact that the voltage of the bus near the fault location deviates the most, to identify the faulty bus. The faulty line is identified using a power differential criterion based on the three-phase differential power.

3.1. Fault Detection and Fault Area Identification

Unbalanced faults occurring in a system can be detected using the negative or zero sequence components of bus voltages [22]. The faulty situation can be identified using the following criteria.

$$|\bar{V}_{b2}| \geq K_2V_N \quad \text{or} \quad |\bar{V}_{b0}| \geq K_0V_N, \tag{6}$$

where \bar{V}_{b2} and \bar{V}_{b0} are the negative and zero sequence components of bth bus respectively in a B-bus system and is the rated voltage magnitude of the bus K_2 and K_0 are the thresholds whose values are selected such that all unbalanced faults in the system can be detected reliably. The occurrence of balanced faults can be identified by positive sequence components of the bus voltages using the criterion given below:

$$|\bar{V}_{b1}| \leq K_1V_N, \tag{7}$$

where \bar{V}_{b1} is the positive sequence component of bth bus and K_1 is the threshold, whose value is appropriately set to identify balanced faults in the system. The values of thresholds K_1 , K_2 and K_0 range between 0 and 1. During fault conditions and normal switching

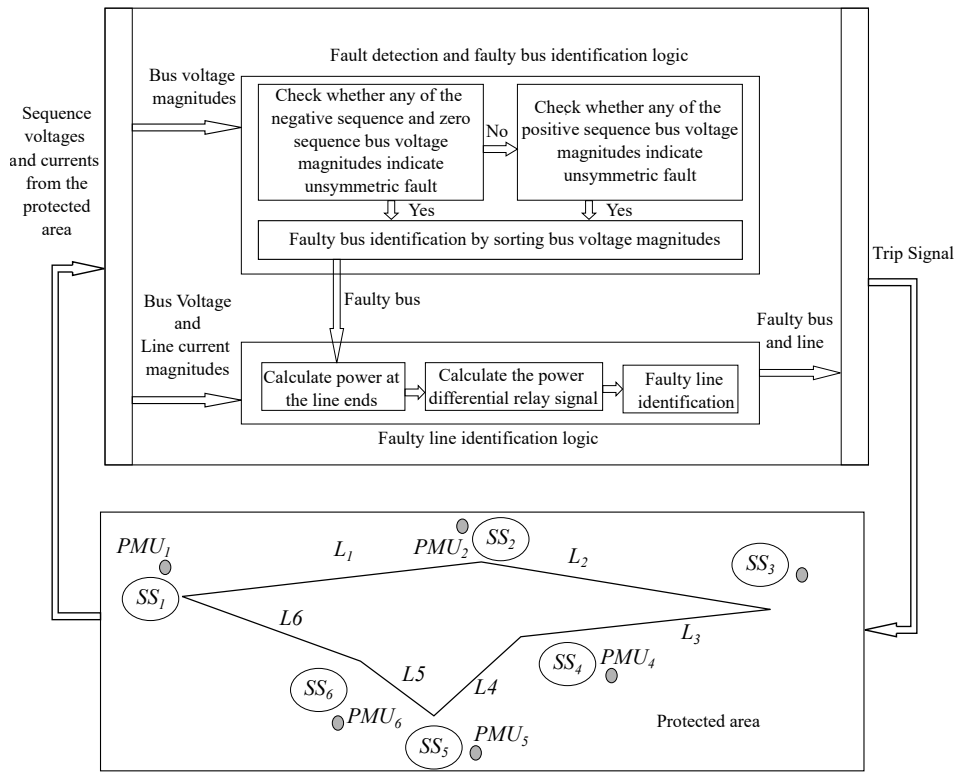


Fig. 2: Schematic diagram of proposed WAMS-based protection scheme.

in of loads \bar{V}_{b1} reduces to lower values from rated value. The reduction is higher during faults. The threshold value K_1 is selected such as to avoid frequent pickup during normal switching of the system. During unsymmetrical fault conditions $|\bar{V}_{b2}|$ and $|\bar{V}_{b0}|$ increases, which are otherwise negligible. Low threshold values of K_2 and K_0 are selected such as to improve high impedance fault sensitivity. The faulty area is identified by sorting the buses in the order of sequence component magnitudes. In the case of an unbalanced fault, the buses are sorted in the descending order of negative sequence bus voltage magnitudes. In the case of balanced fault, the buses are sorted in the ascending order of positive sequence bus voltage magnitudes. The bus at the top of the sorted list is identified as a faulty bus.

3.2. Faulty Line Identification

For faulty line identification, a new criterion based on the three-phase active power differential value is proposed in this section. The schematic of the active power differential relay is shown in Fig. 3. The three-phase differential power of a line connected between buses X and Y is calculated as:

$$Pd_{xy} = |P_{xy} - P_{yx}|, \tag{8}$$

where P_{xy} the three-phase power measured at the line terminal near bus X and P_{yx} is the three-phase power measured at the line terminal near bus Y .

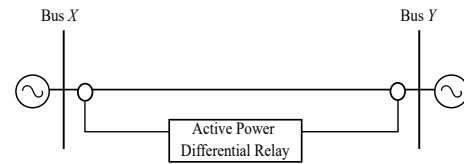


Fig. 3: Active power differential relay schematic.

A high value of differential power Pd_{xy} above the normal line losses in a transmission line is an indication of abnormal current flow in the line. It may be due to an overloaded condition or due to the occurrence of a fault. A threshold value Pd_{xyT} can be set to detect abnormal conditions.

A relaying signal R_{xy} is obtained using the active power differential value as follows:

$$R_{xy} = \frac{Pd_{xy}}{Pr_{xy}}, \tag{9}$$

where

$$Pr_{xy} = \frac{(|P_{xy}| + |P_{yx}|)}{2}. \tag{10}$$

For the normal operating region considering the line loading and load power factor, the value of relaying signal R_{xy} is low for all the lines. When a fault occurs in the system, R_{xy} shoots up to higher values.

As the magnitude R_{xy} depends on the length and line parameters, the normalized value of R_{xy} each

line is used to identify the faulty line. The normalized value is defined as:

$$R_{xy} = \frac{R_{xy}}{R_{xyT}}. \quad (11)$$

where R_{xyT} is the threshold value set for the line and its value is taken as the maximum value of R_{xy} at rated line loading condition considering the normal range of load power factor.

The line with the highest R_{xy} that is connected to the faulty bus is identified as the faulty line. Equation (12) and Eq. (13) are used to compute superimposed components P_{xys} and P_{yxs} of the real power flow at terminals X and Y . It is the difference power between the n th and $(n-1)$ th cycle:

$$P_{xys} = |P_{xy[n^{\text{th}} \text{ cycle}]} - P_{xy[(n-1)^{\text{th}} \text{ cycle}]}, \quad (12)$$

$$P_{yxs} = |P_{yx[n^{\text{th}} \text{ cycle}]} - P_{yx[(n-1)^{\text{th}} \text{ cycle}]}. \quad (13)$$

A sudden change in the value of P_{xys} or P_{yxs} above a threshold P_{xysT} is an indicator of a sudden change in the transmission system and can be used to confirm the occurrence of the fault and to avoid unnecessary pickup at power oscillations.

3.3. Summary of the Proposed WAMS-based Hierarchical Power Differential Algorithm

In the proposed algorithm, the changes in the bus sequence magnitudes, the three-phase differential real power of the transmission lines, and superimposed three-phase real power components at the line ends in each cycle are monitored. The changes in real power flow due to the changes in load demand or due to the change in operating modes of the control devices are slower compared to that due to a sudden fault in the system. The device losses can be included in the transmission line losses while calculating the differential power. The value of superimposed components of real power is an indicator of sudden disturbance in the system. The differential real power in a line and superimposed real power components of the line ends are used to confirm the faulty state of the line. The steps to be followed to identify the faulty line (detailed in Sec. 3.1. and Sec. 3.2.) is summarized below.

Step 1: Collect all the time-synchronized bus voltages and line currents through WAMS.

Step 2: Calculate the sequence components of all bus voltages.

Step 3: Check whether the condition $|\bar{V}_{b2}| \geq K_2 V_N$ or $|\bar{V}_{b0}| \geq K_0 V_N$ is true. If the condition is satisfied,

an unsymmetrical fault is suspected to have occurred in the system and go to step 5 else go to step 4.

Step 4: Check whether the condition $|\bar{V}_{b1}| \geq K_1 V_N$ is true. If the condition is satisfied, a symmetrical fault is suspected to have occurred in the system. Go to step 6 else go to step 1.

Step 5: Sort the negative sequence bus voltages in descending order and find the buses with the highest value of negative sequence voltage magnitude and tag them as the "Faulty/suspicious" buses and go to step 7.

Step 6: Sort the positive sequence bus voltages in ascending order and display, find the buses with the lowest value of positive sequence voltage magnitude and tag them as the "Faulty/suspicious" buses. Go to step 7

Step 7: Calculate the differential power Pd_{xy} (Eq. (8)), relaying signal, R_{xy} (Eq. (11)), and the superimposed power component P_{xys} (Eq. (12)) for all lines connected to the suspicious bus.

Step 8: Identify the faulty line using the hierarchical order of the normalized magnitudes of the signal R_{xy} of the lines in the faulty area.

Step 9: Check whether:

1. The magnitude of differential power is greater than the threshold value Pd_{xyT} .
2. The magnitude of superimposed power components in the line is greater than the threshold value P_{sT} .
3. The value of R_{xy} falls in the faulty region of the line characteristics (ie R_{xy} is greater than R_{xyT}). If all the above conditions are satisfied for any of the lines connected to the "Faulty/suspicious bus" go to step 10, else go to step 1.

Step 10: The fault is confirmed, the faulty line number is displayed and appropriate protective actions are initiated. Go to step1.

The algorithm is depicted in the flow chart in Fig. 4.

4. Validation of the Proposed Algorithm

The proposed WAMS-based algorithm is validated through simulation under MATLAB/SIMULINK environment. Simulation studies are carried out on a modified WSCC 9 bus system incorporating a FACTS device at the midpoint of the line connecting buses 7 and 8 as shown in Fig. 5.

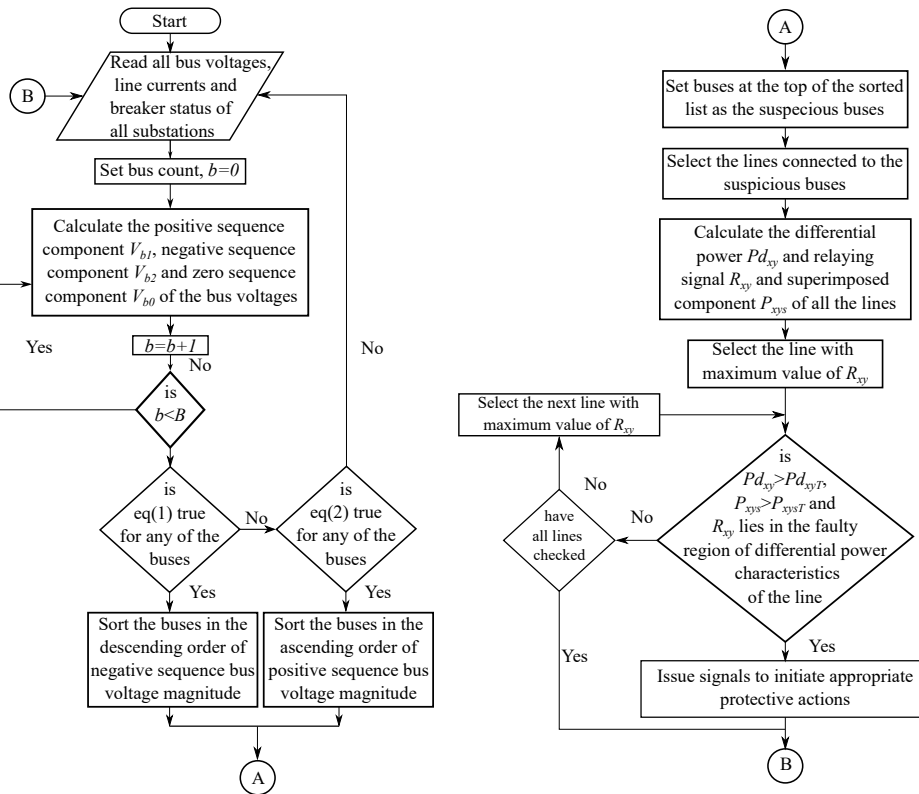


Fig. 4: Flow chart of the proposed WAMS-based hierarchical active power differential relaying signal-based algorithm.

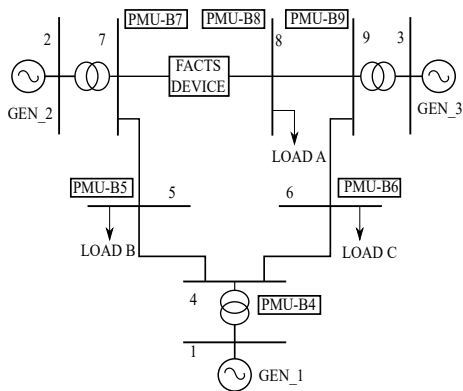


Fig. 5: Modified WSCC 9 bus system - single line diagram including FACTS device at the midpoint of line connected between bus 7 and bus 8.

The values of thresholds are set as follows $K_1 = 0.6$, $K_2 = K_0 = 0.1$. The values of Pd_{xyT} and R_{xyT} are set according to the normal value of line losses and power differential characteristics of each line. The system is operated at normal operating conditions and the threshold values Pd_{xyT} and R_{xyT} for different lines are identified and shown in Tab. 1.

Variation of superimposed components of active power P_{xys} during the fault is used to confirm a sudden change in the power flow through the line. $P_{sT} = 0.05$ pu selected as a common threshold for all lines to confirm the occurrence of a fault. The value

Tab. 1: Threshold values selected for different lines.

Line	Pd_{xyT} (pu value on a common base of 400 MVA)	R_{xyT}
Line 7–8	0.03	0.015
Line 8–9	0.025	0.02
Line 9–6	0.022	0.022
Line 6–4	0.026	0.014
Line 4–5	0.026	0.014
Line 5–7	0.022	0.022

depends on the possible change of power in one cycle during the normal operation of the system.

Typical types of faults are simulated at various distances with different fault resistances varying from 1 to 500 Ω . The algorithm is validated by placing SVC, TCSC, SSSC, and STATCOM at the midpoint of line 7–8. Variations of P_{xy} , and P_{xys} are shown in Fig. 6.

4.1. Simulation Results for a Fault on Line 7–8 with Different FACTS Devices on Line 7–8

Faults are created at $t = 2$ s on line 7–8 placing different FACTS devices on the same line. Possible combinations of various FACTS devices with varying fault types, fault distance, and fault resistance are simulated to validate the performance of the proposed

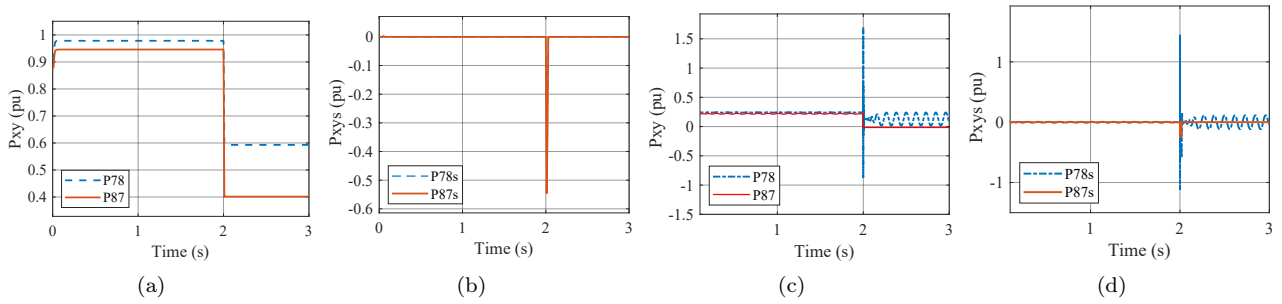


Fig. 6: Variation of P_{xy} , and P_{xyS} signal for a fault in Line 7–8. (a) and (b) LG fault near bus 8 when the line is heavily loaded in the presence of STATCOM. (c) and (d) LLLG fault near bus 8 when the line is lightly loaded in the presence of SSSC.

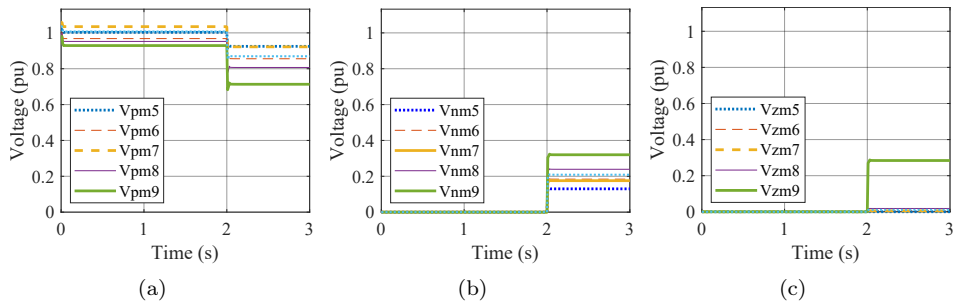


Fig. 7: Case A1: Variation of magnitudes of (a) positive sequence, (b) negative sequence and (c) zero-sequence bus voltages for an LG fault at $t = 2$ s near bus 8 in line 7–8 containing STATCOM.

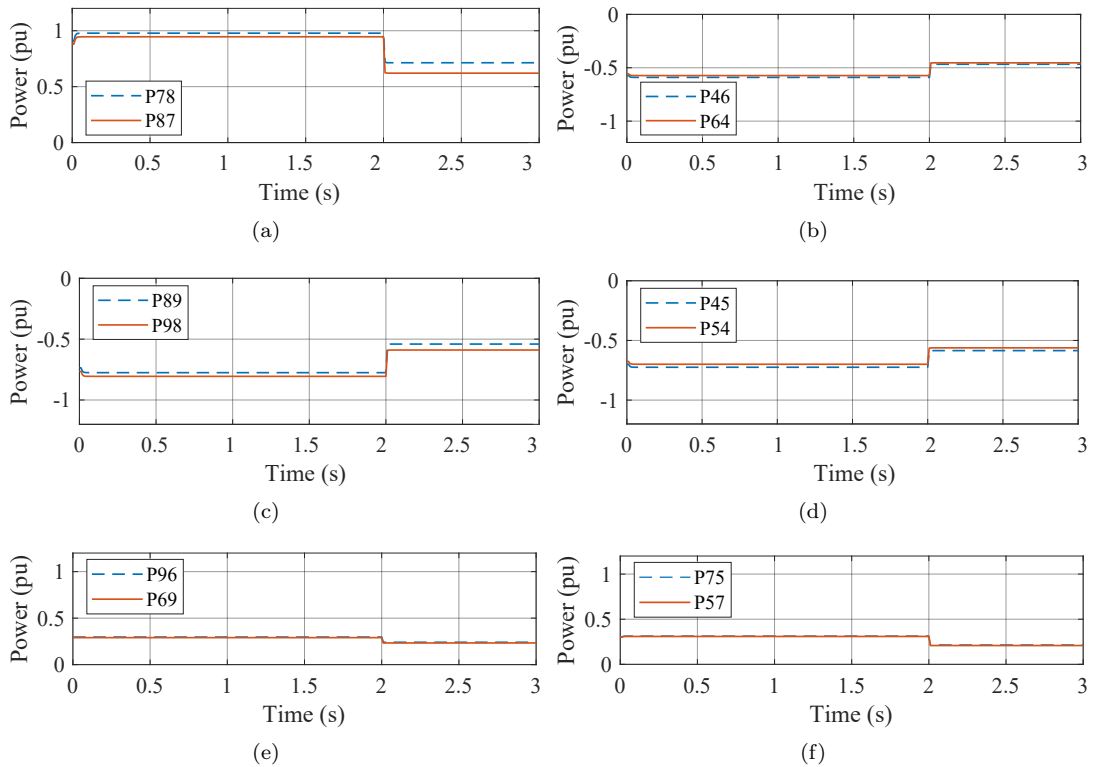


Fig. 8: Case A1: Variation of P_{xy} in different lines for an LG fault near bus 8 in line 7–8 containing STATCOM.

algorithm. Four typical cases are demonstrated here, namely:

- Case A1: Fault Type: LG, FACTS device: STATCOM.
- Case A2: Fault Type: LL, FACTS device: TCSC.
- Case A3: Fault Type: LLLG, FACTS device: SSSC.
- Case A4: Fault Type: LLG, FACTS device: SVC.

When the occurrence of a fault is detected in the system, the suspicious bus is selected based on the magnitudes of bus voltage sequence components. The values of Pd_{xy} and R_{xy} are calculated for all the lines connected to the suspicious bus. The line with maximum \tilde{R}_{xy} satisfying the threshold conditions is identified as the faulty line.

Case A1: Fault Type: LG, FACTS device: STATCOM.

An LG fault with ground resistance 10Ω is simulated at line 7–8 near bus 8. Variation of bus voltage sequence components and line end powers during the simulation periods are shown in Fig. 7 and Fig. 8 respectively. The magnitude of negative sequence bus voltage has the highest value for bus 8, and its value is above the threshold set. This confirms the occurrence of an asymmetrical fault in a line connected to bus 8. The algorithm compares the values of \tilde{R}_{xy} of the lines connected to bus 8. The magnitude of \tilde{R}_{78} is the highest after the fault as shown in Fig. 9 and line 7–8 is identified as the faulty line. The occurrence of the fault on line 7–8 is confirmed by the change in superimposed components.

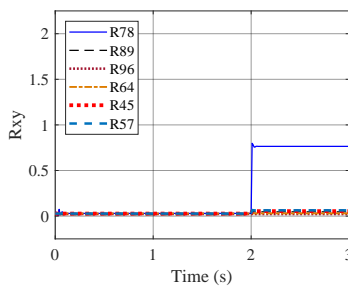


Fig. 9: Case A1: Variation of R_{xy} for various lines (R_{78} , R_{89} , R_{96} , R_{64} , R_{45} , R_{57}) for an LG fault ($R_f = 10 \Omega$) at $t = 2$ s near bus 7 on line 7–8 with STATCOM in line 7–8.

Case A2: Fault Type: LL, FACTS device: TCSC.

A line-to-line fault with 0.1Ω is created at line 7–8 near bus 7 at $t = 2$ s. Line 7–8 contains TCSC. Bus 7 is identified as the faulty bus as the negative sequence bus voltage of bus 7 satisfies the criterion. The magnitude of \tilde{R}_{78} is the highest as in Fig. 10. So, line 7–8 is identified as the faulty line.

Case A3: Fault Type: LLLG, FACTS device: SSSC.

An LLLG fault with ground resistance of 10Ω is simulated near bus 8. The occurrence of a symmetrical fault on a line connected to bus 8 is confirmed according to the faulty bus identification steps. The magnitude \tilde{R}_{78} is the highest after the fault (Fig. 11) and indicates a fault in line 7–8.

Case A4: Fault Type: LLG, FACTS device: SVC.

An LLG fault with ground resistance 100Ω is simulated near bus 7. An asymmetrical fault on a line connected to bus 7 is identified. The magnitude \tilde{R}_{78} is the highest after the fault (Fig. 12) and line 7–8 is identified as the faulty one. The results of different cases simulated are summarized in Tab. 2.

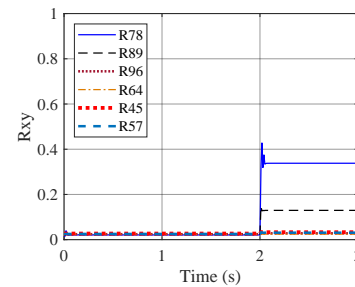


Fig. 10: Case A2: Variation of R_{xy} for various lines (R_{78} , R_{89} , R_{96} , R_{64} , R_{45} , R_{57}) for an LL fault ($R_f = 0.1 \Omega$) at $t = 2$ s on line 7–8 near bus 8 with TCSC on line 7–8.

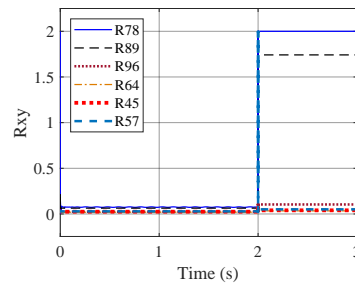


Fig. 11: Case A3: Variation of R_{xy} for various lines (R_{78} , R_{89} , R_{96} , R_{64} , R_{45} , R_{57}) for an LLLG fault ($R_f = 10 \Omega$) at $t = 2$ s near bus 8 on line 7–8 with SSSC in line 7–8.

4.2. Simulation Results for a Fault on Line Other than Line 7–8 with Different FACTS Devices in Line 7–8

In this case, different FACTS devices are placed on line 7–8. Faults are created on other lines in the system. It is observed that the algorithm identifies the faulty line reliably in these cases also. Four typical cases are demonstrated here, namely:

Tab. 2: Performance of the algorithm for a fault on line 7–8.

FACTS device in line 7–8	Faulty bus and line	Fault type	Fault resistance	Line and bus identified
STATCOM	Bus 7 Line 7–8	LG	1, 10, 100, 500	Bus 7, Line 7–8
	Bus 8, Line 7–8	LG	1, 10, 100, 500	Bus 8, Line 7–8
	Bus 7, Line 7–8	LLG	1, 10, 100, 500	Bus 7, Line 7–8
	Bus 8, Line 7–8	LLG	1, 10, 100, 500	Bus 8, Line 7–8
	Bus 7, Line 7–8	LLLG	1, 10, 100, 500	Bus 7, Line 7–8
	Bus 8, Line 7–8	LLLG	1, 10, 100, 500	Bus 8, Line 7–8
	Bus 7, Line 7–8	LL	0.1, 1, 10	Bus 7, Line 7–8
	Bus 8, Line 7–8	LL	0.1, 1, 10	Bus 8, Line 7–8
	Bus 7, Line 7–8	LLL	0.1, 1, 10	Bus 7, Line 7–8
SVC	Bus 8, Line 7–8	LLL	0.1, 1, 10	Bus 8, Line 7–8
	Bus 7, Line 7–8	LG	1, 10, 100, 500	Bus 7, Line 7–8
	Bus 8, Line 7–8	LG	1, 10, 100, 500	Bus 8, Line 7–8
	Bus 7, Line 7–8	LLG	1, 10, 100, 500	Bus 7, Line 7–8
	Bus 8, Line 7–8	LLG	1, 10, 100, 500	Bus 8, Line 7–8
	Bus 7, Line 7–8	LLLG	1, 10, 100, 500	Bus 7, Line 7–8
	Bus 8, Line 7–8	LLLG	1, 10, 100, 500	Bus 8, Line 7–8
	Bus 7, Line 7–8	LL	0.1, 1, 10	Bus 7, Line 7–8
	Bus 8, Line 7–8	LL	0.1, 1, 10	Bus 8, Line 7–8
SSSC	Bus 7, Line 7–8	LLL	0.1, 1, 10	Bus 7, Line 7–8
	Bus 8, Line 7–8	LLL	0.1, 1, 10	Bus 8, Line 7–8
	Bus 7, Line 7–8	LG	1, 10, 100, 500	Bus 7, Line 7–8
	Bus 8, Line 7–8	LG	1, 10, 100, 500	Bus 8, Line 7–8
	Bus 7, Line 7–8	LLG	1, 10, 100, 500	Bus 7, Line 7–8
	Bus 8, Line 7–8	LLG	1, 10, 100, 500	Bus 8, Line 7–8
	Bus 7, Line 7–8	LLLG	1, 10, 100, 500	Bus 7, Line 7–8
	Bus 8, Line 7–8	LLLG	1, 10, 100, 500	Bus 8, Line 7–8
	Bus 7, Line 7–8	LL	0.1, 1, 10	Bus 7, Line 7–8
TCSC	Bus 8, Line 7–8	LL	0.1, 1, 10	Bus 8, Line 7–8
	Bus 7, Line 7–8	LL	0.1, 1, 10	Bus 7, Line 7–8
	Bus 7, Line 7–8	LLL	0.1, 1, 10	Bus 7, Line 7–8
	Bus 8, Line 7–8	LLL	0.1, 1, 10	Bus 8, Line 7–8
	Bus 7, Line 7–8	LG	1, 10, 100, 500	Bus 7, Line 7–8
	Bus 8, Line 7–8	LG	1, 10, 100, 500	Bus 8, Line 7–8
	Bus 7, Line 7–8	LLG	1, 10, 100, 500	Bus 7, Line 7–8
	Bus 8, Line 7–8	LLG	1, 10, 100, 500	Bus 8, Line 7–8
	Bus 7, Line 7–8	LLLG	1, 10, 100, 500	Bus 7, Line 7–8

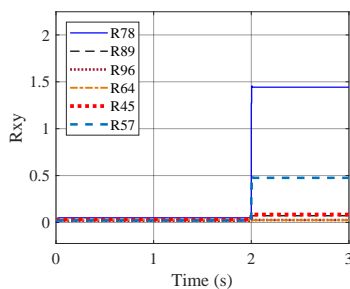


Fig. 12: Case A4: Variation of R_{xy} for various lines (R_{78} , R_{89} , R_{96} , R_{64} , R_{45} , R_{57}) for an LLG fault ($R_f = 100 \Omega$) at $t = 2$ s near bus 7 on line 7–8 with SVC in line 7–8.

- Case B1: Fault Type: LLL, Line: 8–9 FACTS device: SSSC.
- Case B2: Fault Type: LL, Line:6–4 FACTS device: STATCOM.
- Case B3: Fault Type: LG, Line: 5–7 FACTS device: SVC.

- Case B4: Fault Type: LLG, Line: 9–6 FACTS device: TCSC.

Case B1: Fault Type: LLL, Line:8–9 FACTS device: SSSC.

Variations of bus voltage sequence components and line end powers during the simulation periods are shown in Fig. 13 and Fig. 14 respectively for an LLL fault, with fault resistance 1Ω , near bus 9 in Line 8–9. Magnitudes of negative and zero sequence components are negligible for symmetric faults. The magnitude of positive sequence bus voltage is the lowest for bus 9 and is below the threshold value. This indicates the occurrence of a symmetrical fault on a line connected to bus 9. The magnitude of \tilde{R}_{89} is the highest after the fault as shown in Fig. 15 and line 7–8 is identified as the faulty line.

Case B2: Fault Type and line: LL fault at line 6–4, FACTS device: STATCOM.

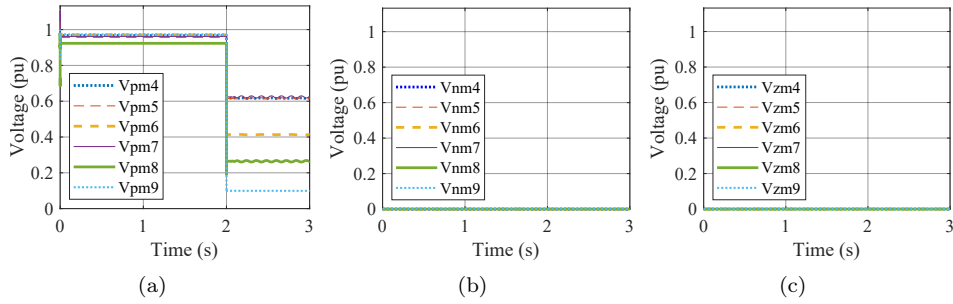


Fig. 13: Case B1: Variation of magnitudes of (a) positive sequence, (b) negative sequence and (c) zero-sequence bus voltages for an LLL fault near bus 9 in line 8–9 containing SSSC (Magnitudes of negative and zero sequence components are negligible for symmetric faults).

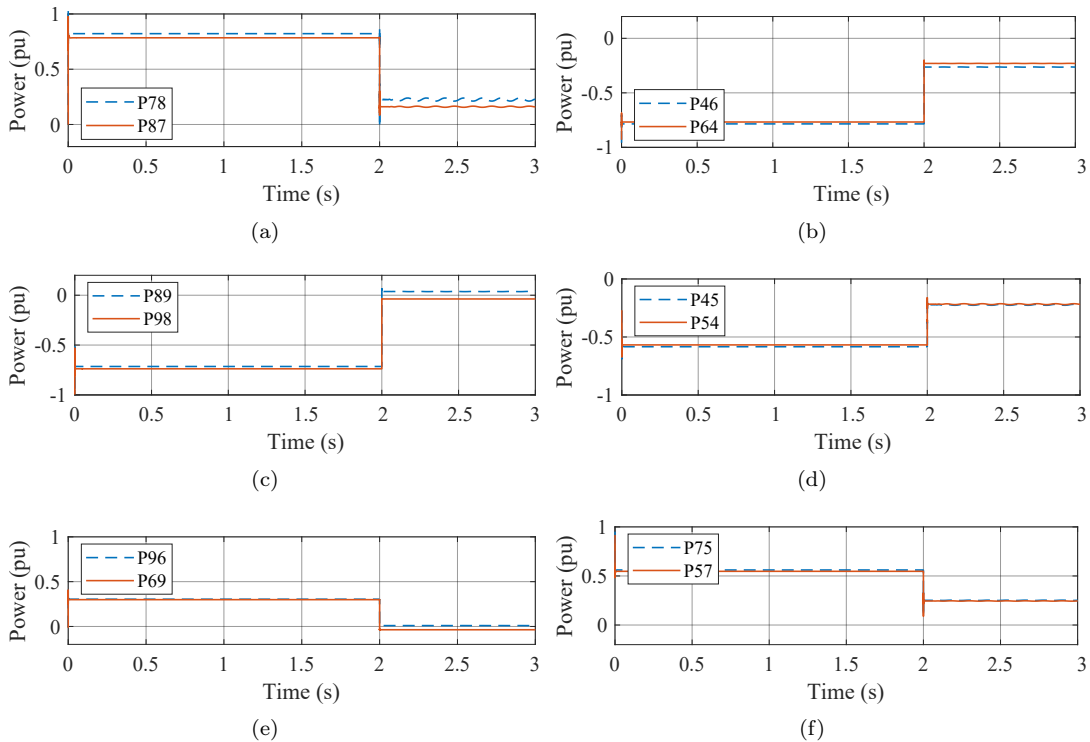


Fig. 14: Case B1: Variation of P_{xy} for an LLL fault near bus 9 in line 8–9 containing SSSC.

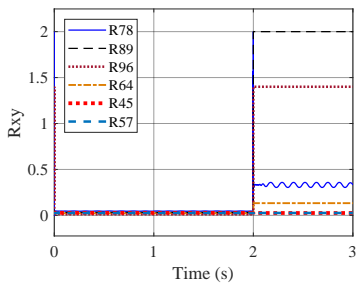


Fig. 15: Case B1: Variation of R_{xy} for various lines (R_{78} , R_{89} , R_{96} , R_{64} , R_{45} , R_{57}) for an LLL fault ($R_f = 1 \Omega$) at $t = 2$ s near bus 9 on line 8–9 with SSSC in line 7–8.

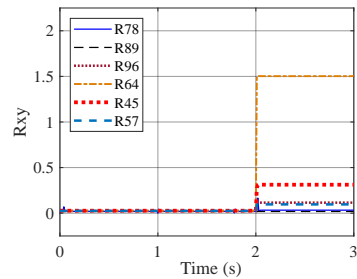


Fig. 16: Case B2: Variation of R_{xy} for various lines (R_{78} , R_{89} , R_{96} , R_{64} , R_{45} , R_{57}) for an LL fault ($R_f = 10 \Omega$) at $t = 2$ s near bus 4 on line 6–4 with STATCOM on line 7–8.

Tab. 3: Performance of the algorithm for a fault on a line other than line 7–8.

FACTS device in line 7–8	Faulty bus and line	Fault type	Fault resistance	Line and bus identified
STATCOM	Bus 7, Line 7–5	LG	1, 10, 100, 500	Bus 7, Line 7–5
	Bus 5, Line 7–5	LG	1, 10, 100, 500	Bus 5, Line 7–5
	Bus 5, Line 5–4	LLG	1, 10, 100, 500	Bus 5, Line 5–4
	Bus 4, Line 5–4	LLG	1, 10, 100, 500	Bus 4, Line 5–4
	Bus 4, Line 4–6	LLLG	1, 10, 100, 500	Bus 4, Line 4–6
	Bus 6, Line 4–6	LLLG	1, 10, 100, 500	Bus 6, Line 4–6
	Bus 6, Line 9–6	LL	0.1, 1, 10	Bus 6, Line 9–6
	Bus 9, Line 9–6	LL	0.1, 1, 10	Bus 9, Line 9–6
	Bus 9, Line 8–9	LLL	0.1, 1, 10	Bus 9, Line 8–9
SVC	Bus 8, Line 8–9	LLL	0.1, 1, 10	Bus 8, Line 8–9
	Bus 7, Line 7–5	LG	1, 10, 100, 500	Bus 7, Line 7–5
	Bus 5, Line 7–5	LG	1, 10, 100, 500	Bus 5, Line 7–5
	Bus 5, Line 5–4	LLG	1, 10, 100, 500	Bus 5, Line 5–4
	Bus 4, Line 5–4	LLG	1, 10, 100, 500	Bus 4, Line 5–4
	Bus 4, Line 4–6	LLLG	1, 10, 100, 500	Bus 4, Line 4–6
	Bus 6, Line 4–6	LLLG	1, 10, 100, 500	Bus 6, Line 4–6
	Bus 6, Line 9–6	LL	0.1, 1, 10	Bus 6, Line 9–6
	Bus 9, Line 9–6	LL	0.1, 1, 10	Bus 9, Line 9–6
SSSC	Bus 9, Line 8–9	LLL	0.1, 1, 10	Bus 9, Line 8–9
	Bus 8, Line 8–9	LLL	0.1, 1, 10	Bus 8, Line 8–9
	Bus 7, Line 7–5	LG	1, 10, 100, 500	Bus 7, Line 7–5
	Bus 5, Line 7–5	LG	1, 10, 100, 500	Bus 5, Line 7–5
	Bus 5, Line 5–4	LLG	1, 10, 100, 500	Bus 5, Line 5–4
	Bus 4, Line 5–4	LLG	1, 10, 100, 500	Bus 4, Line 5–4
	Bus 4, Line 4–6	LLLG	1, 10, 100, 500	Bus 4, Line 4–6
	Bus 6, Line 4–6	LLLG	1, 10, 100, 500	Bus 6, Line 4–6
	Bus 6, Line 9–6	LL	0.1, 1, 10	Bus 6, Line 9–6
TCSC	Bus 9, Line 9–6	LL	0.1, 1, 10	Bus 9, Line 9–6
	Bus 9, Line 8–9	LLL	0.1, 1, 10	Bus 9, Line 8–9
	Bus 8, Line 8–9	LLL	0.1, 1, 10	Bus 8, Line 8–9
	Bus 7, Line 7–5	LG	1, 10, 100, 500	Bus 7, Line 7–5
	Bus 5, Line 7–5	LG	1, 10, 100, 500	Bus 5, Line 7–5
	Bus 5, Line 5–4	LLG	1, 10, 100, 500	Bus 5, Line 5–4
	Bus 4, Line 5–4	LLG	1, 10, 100, 500	Bus 4, Line 5–4
	Bus 4, Line 4–6	LLLG	1, 10, 100, 500	Bus 4, Line 4–6
	Bus 6, Line 4–6	LLLG	1, 10, 100, 500	Bus 6, Line 4–6

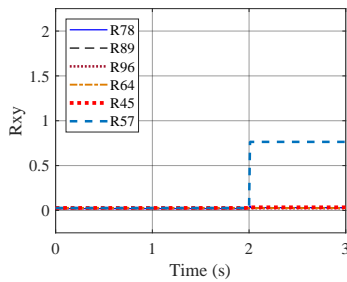


Fig. 17: Case B3: Variation of R_{xy} for various lines for an LG fault ($R_f = 500 \Omega$) at $t = 2$ s near bus 7 on line 5–7 with SVC on Line 7–8.

An LL fault near bus 4 at line 6–4 is simulated with STATCOM on line 7–8 and fault resistance 10Ω . The magnitude of negative sequence bus voltage is found maximum for bus 4. It is identified as the faulty bus. The magnitude of \tilde{R}_{64} is observed as the highest as shown in Fig. 16 and line 6–4 is confirmed as the faulty line.

Case B3: Fault Type: LG fault at line 5–7 FACTS device: SVC.

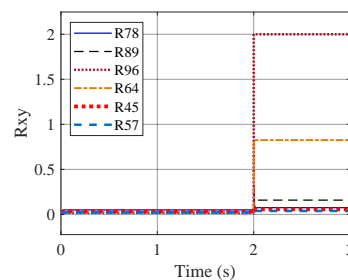


Fig. 18: Case B4: Variation of R_{xy} for various lines for an LLG fault ($R_f = 1 \Omega$) at $t = 2$ s near bus 6 on line 9–6 with TCSC on line 7.

LG fault is created in line 5–7 with ground resistance of 500Ω near bus 7. Bus 7 is successfully identified as the faulty bus. Line 5–7 is identified as faulty with the highest value of \tilde{R}_{57} (Fig. 17).

Case B4: Fault Type: LLG fault at line 9–6 FACTS device: TCSC.

In line 9–6, an LG fault is created near bus 6 ground resistance 1Ω . Line 7–8 has a TCSC at the midpoint. After the fault, bus 6 has the negative sequence bus voltage above the threshold set and is the highest. Bus 6 is detected as the faulty bus. \tilde{R}_{96} has the highest value indicating a fault in line 9–6 (Fig. 18). The results are summarized in Tab. 3.

5. Conclusion

A WAMS-based generalized backup protection algorithm, for a transmission system containing mid-point FACTS compensated lines, is developed using the active power differential principle. The active power differential value is not affected by the compensating device operation, either series or shunt. So, it is more appropriate for generalized relaying purposes compared to the current differential signal. The compensating device cannot exchange active power on its own with the transmission line, unless it is supported by an active power source that can supply and absorb active power. The threshold settings are so adjusted to overcome the device losses.

The proposed algorithm is validated on a Modified WSCC 9 Bus system, incorporating FACTS devices, through simulation studies in MATLAB/SIMULINK environment. Symmetrical and unsymmetrical faults are simulated on different lines in the system. Various types of faults are created with different fault parameters to verify the effectiveness of the algorithm. The proposed WAMS-based algorithm successfully identifies the faulty line in all these cases. The proposed backup protection scheme can support the primary distance protection of the transmission system and does not depend on the apparent impedance. This algorithm can identify faulty buses and lines in a system containing compensated and uncompensated lines. It can be used in both series and shunt compensated systems. Fault type, fault parameters, and line loading do not affect the performance of the algorithm. The Algorithm identifies the line in a period of 2–4 cycles, Considering the communication delay in the system a worst case of 9 to 11 cycles, can be expected for the protective actions, which is a reasonable time delay that can be allowed for backup protection.

Author Contributions

S.V. developed the theoretical formalism, performed the analytic calculations, and performed the numerical simulations. Both P.A. and S.R.A. contributed

to the final version of the manuscript. P.A. supervised the project.

References

- [1] HINGORANL, N. G. *Understanding FACTS*. 1st ed. Hoboken: John Wiley & Sons, 2000. ISBN 978-0-7803-3455-7.
- [2] BISWAS, S. and P. K. NAYAK. State-of-the-art on the protection of FACTS compensated high-voltage transmission lines: a review. *High Voltage*. 2018, vol. 3, iss. 1, pp. 21–30. ISSN 2397-7264. DOI: 10.1049/hve.2017.0131.
- [3] KHEDERZADEH, M. and A. GHORBANI. Impact of VSC-Based Multiline FACTS Controllers on Distance Protection of Transmission Lines. *IEEE Transactions on Power Delivery*. 2012, vol. 27, iss. 1, pp. 32–39. ISSN 1937-4208. DOI: 10.1109/TPWRD.2011.2168428.
- [4] PHADKE, A. G. Synchronized phasor measurements in power systems. *IEEE Computer Applications in Power*. 1993, vol. 6, iss. 2, pp. 10–15. ISSN 1558-4151. DOI: 10.1109/67.207465.
- [5] CROSSLEY, P. A. and P. G. MCLAREN. Distance Protection Based on Traveling Waves. *IEEE Transactions on Power Apparatus and Systems*. 1983, vol. 102, iss. 9, pp. 2971–2983. ISSN 0018-9510. DOI: 10.1109/TPAS.1983.318102.
- [6] SHEHAB-ELDIN, E. H. and P. G. MCLAREN. Travelling wave distance protection-problem areas and solutions. *IEEE Transactions on Power Delivery*. 1988, vol. 3, iss. 3, pp. 894–902. ISSN 1937-4208. DOI: 10.1109/61.193866.
- [7] KORKALI, M., H. LEV-ARI and A. ABUR. Traveling-Wave-Based Fault-Location Technique for Transmission Grids Via Wide-Area Synchronized Voltage Measurements. *IEEE Transactions on Power Systems*. 2012, vol. 27, iss. 2, pp. 1003–1011. ISSN 1558-0679. DOI: 10.1109/TPWRS.2011.2176351.
- [8] JOHNS, A. T. and P. AGRAWAL. New approach to power line protection based upon the detection of fault induced high frequency signals. *IEE Proceedings C Generation, Transmission and Distribution*. 1990, vol. 137, iss. 4, pp. 307. ISSN 2053-7921. DOI: 10.1049/ip-c.1990.0041.
- [9] BO, Z. Q., M. A. REDFERN and G. C. WELLER. Positional protection of transmission line using fault generated high frequency transient signals. *IEEE Transactions on Power Delivery*. 2000,

- vol. 15, iss. 3, pp. 888–894. ISSN 1937-4208. DOI: 10.1109/61.871348.
- [10] SERIZAWA, Y., M. MYOUJIN, K. KITAMURA, N. SUGAYA, M. HORI, A. TAKEUCHI, I. SHUTO and M. INUKAI. Wide-area current differential backup protection employing broadband communications and time transfer systems. *IEEE Transactions on Power Delivery*. 1998, vol. 13, iss. 4, pp. 1046–1052. ISSN 1937-4208. DOI: 10.1109/61.714445.
- [11] HALL, I., P. G. BEAUMONT, G. P. BABER, I. SHUTO, M. SAGA, K. OKUNO and H. ITO. New line current differential rehav using gps synchronization. In: *2003 IEEE Bologna Power Tech Conference Proceedings*. Bologna: IEEE, 2003, pp. 670–677. ISBN 978-0-7803-7967-1. DOI: 10.1109/PTC.2003.1304464.
- [12] VOLOH, I. and Z. ZHANG. Fault locator based on line current differential relays synchronized measurements. In: *2010 63rd Annual Conference for Protective Relay Engineers*. College Station: IEEE, 2010, pp. 1–13. ISBN 978-1-4244-6073-1. DOI: 10.1109/CPRE.2010.5469521.
- [13] KEZUNOVIC, M. and B. PERUNICIC. Automated transmission line fault analysis using synchronized sampling at two ends. *IEEE Transactions on Power Systems*. 1996, vol. 11, iss. 1, pp. 441–447. ISSN 1558-0679. DOI: 10.1109/59.486131.
- [14] EISSA, M. M. and O. P. MALIK. A new digital directional transverse differential current protection technique. *IEEE Transactions on Power Delivery*. 1996, vol. 11, iss. 3, pp. 1285–1291. ISSN 1937-4208. DOI: 10.1109/61.517482.
- [15] JIANG, J.-A., J.-Z. YANG, Y.-H. LIN, C.-W. LIU and J.-C. MA. An adaptive PMU based fault detection/location technique for transmission lines. I. Theory and algorithms. *IEEE Transactions on Power Delivery*. 2000, vol. 15, iss. 2, pp. 486–493. ISSN 1937-4208. DOI: 10.1109/61.852973.
- [16] JIANG, J.-A., C.-S. CHEN and C.-W. LIU. A new protection scheme for fault detection, direction discrimination, classification, and location in transmission lines. *IEEE Transactions on Power Delivery*. 2003, vol. 18, iss. 1, pp. 34–42. ISSN 1937-4208. DOI: 10.1109/TPWRD.2002.803726.
- [17] HE, Z., Z. ZHANG, W. CHEN, O. P. MALIK and X. YIN. Wide-Area Backup Protection Algorithm Based on Fault Component Voltage Distribution. *IEEE Transactions on Power Delivery*. 2011, vol. 26, iss. 4, pp. 2752–2760. ISSN 1937-4208. DOI: 10.1109/TPWRD.2011.2165971.
- [18] EISSA, M. M., M. E. MASOUD and M. M. M. ELANWAR. A Novel Back Up Wide Area Protection Technique for Power Transmission Grids Using Phasor Measurement Unit. *IEEE Transactions on Power Delivery*. 2010, vol. 25, iss. 1, pp. 270–278. ISSN 1937-4208. DOI: 10.1109/TPWRD.2009.2035394.
- [19] MA, J., J. LI, J. S. THORP, A. J. ARANA, Q. YANG and A. G. PHADKE. A Fault Steady State Component-Based Wide Area Backup Protection Algorithm. *IEEE Transactions on Smart Grid*. 2011, vol. 2, iss. 3, pp. 468–475. ISSN 1949-3061. DOI: 10.1109/TSG.2011.2158861.
- [20] NAMDARI, F., S. JAMALI and P. A. CROSSLLEY. Power differential based wide area protection. *Electric Power Systems Research*. 2007, vol. 77, iss. 12, pp. 1541–1551. ISSN 0378-7796. DOI: 10.1016/j.epsr.2006.10.018.
- [21] NAVALKAR, P. V. and S. A. SOMAN. Secure Remote Backup Protection of Transmission Lines Using Synchrophasors. *IEEE Transactions on Power Delivery*. 2011, vol. 26, iss. 1, pp. 87–96. ISSN 1937-4208. DOI: 10.1109/TPWRD.2010.2076350.
- [22] NAYAK, P. K., A. K. PRADHAN and P. BAJPAI. Wide-Area Measurement-Based Backup Protection for Power Network With Series Compensation. *IEEE Transactions on Power Delivery*. 2014, vol. 29, iss. 4, pp. 1970–1977. ISSN 1937-4208. DOI: 10.1109/TPWRD.2013.2294183.
- [23] JENA, M. K., S. R. SAMANTARAY and B. K. PANIGRAHI. A New Wide-Area Backup Protection Scheme for Series-Compensated Transmission System. *IEEE Systems Journal*. 2017, vol. 11, iss. 3, pp. 1877–1887. ISSN 1937-9234. DOI: 10.1109/JSYST.2015.2467218.
- [24] MISHRA, S. K., L. N. TRIPATHY and S. C. SWAIN. A DWT based differential relaying scheme of SVC compensated line. In: *2017 International Conference on Innovative Mechanisms for Industry Applications (ICIMIA)*. Bangalore: IEEE, 2017, pp. 295–301. ISBN 978-1-5090-5960-7. DOI: 10.1109/ICIMIA.2017.7975622.
- [25] KHADKE, P., N. PATNE, A. SINGH and G. SHINDE. Pilot Relaying Scheme Based on Differential Admittance Concept for FSC-Compensated EHV Transmission Line. *Iranian Journal of Science and Technology, Transactions of Electrical Engineering*. 2020, vol. 44, iss. 2, pp. 949–961. ISSN 2364-1827. DOI: 10.1007/s40998-019-00279-3.

- [26] BISWAS, S. and P. K. NAYAK. Superimposed Component-Based Protection Scheme for UPFC Compensated Transmission Lines. In: *2018 20th National Power Systems Conference (NPSC)*. Tiruchirappalli: IEEE, 2018, pp. 1–6. ISBN 978-1-5386-6159-8. DOI: 10.1109/NPSC.2018.8771805.
- [27] KHEDERZADEH, M. Application of synchrophasors to adaptive protection of transmission lines compensated by UPFC. In: *10th IET International Conference on Developments in Power System Protection (DPSP 2010). Managing the Change*. Manchester: IET, 2010, pp. 112–112. ISBN 978-1-84919-212-5. DOI: 10.1049/cp.2010.0256.
- [28] MALLIKARJUNA, B., A. SAGGURTHI, M. J. B. REDDY and D. K. MOHANTA. PMU based Distance Protection Methodology to Avert Malfunction due to FACTS controllers. In: *2018 20th National Power Systems Conference (NPSC)*. Tiruchirappalli: IEEE, 2018, pp. 1–6. ISBN 978-1-5386-6159-8. DOI: 10.1109/NPSC.2018.8771751.
- [29] KUMAR, B. and A. YADAV. Backup protection scheme for transmission line compensated with UPFC during high impedance faults and dynamic situations. *IET Science, Measurement & Technology*. 2017, vol. 11, iss. 6, pp. 703–712. ISSN 1751-8830. DOI: 10.1049/iet-smt.2016.0458.
- [30] ABASI, M., A. SAFFARIAN, M. JOORABIAN and S. G. SEIFOSSADAT. Fault classification and fault area detection in GUPFC-compensated double-circuit transmission lines based on the analysis of active and reactive powers measured by PMUs. *Measurement*. 2021, vol. 169, iss. 1, pp. 1–23. ISSN 0263-2241. DOI: 10.1016/j.measurement.2020.108499.

About Authors

Sreelekha VENUGOPAL received her bachelor's degree in Electrical and Electronics Engineering from Rajiv Gandhi Institute of Technology, Kottayam, India, in 2001. She received her master's from College of Engineering, Trivandrum,

India, in 2003. She joined Rajiv Gandhi Institute of Technology, Kottayam, India, as an Assistant Professor in the Electrical Engineering department, in 2011. She is currently pursuing her Ph.D. at Rajiv Gandhi Institute of Technology, Kottayam, India affiliated with Avul Pakir Jainulabdeen (APJ) Abdul Kalam Technological University, Kerala. Her research interests include power systems, wide-area measurements, smart grids, and microgrids.

Prince ASOK received his bachelor's degree in Electrical and Electronics Engineering from Thanagal Kunju Musaliar (TKM) College of Engineering Kollam, India, in 1996. He received master's and Ph.D. degrees in Electrical Engineering from the Indian Institute of Technology Delhi, New Delhi, India in 2005 and 2012 respectively. He is currently a Professor in the Electrical Engineering Department of Rajiv Gandhi Institute of Technology, Kottayam, India. He is a senior member of Institute of Electrical and Electronics Engineers (IEEE). His research interests include power systems, renewable energy systems, wind energy conversion systems, wide-area measurements, electric vehicles, and signal processing applications in power systems.

Sabha Raj ARYA received the bachelor of Engineering degree in Electrical Engineering from the Government Engineering College Jabalpur, Jabalpur, India, in 2002, the master of technology degree in power electronics from the Motilal National Institute of Technology, Allahabad, India, in 2004, and the Ph.D. degree in Electrical Engineering from the Indian Institute of Technology Delhi, New Delhi, India, in 2014. He is currently an Associate Professor with the Department of Electrical Engineering, Sardar Vallabhbhai National Institute of Technology Surat, Surat, India. He was a recipient of two national awards, namely INAE Young Engineer Award from the Indian National Academy of Engineering, and the Power System Operation Corporation Limited (POSOCO) Power System Award from the Power Grid Corporation of India in the year 2014 for his research work. He is a senior member of IEEE, a member of Institution of Electronics and Telecommunication Engineers (IETE), Systems Society of India, and the Institution of Engineers India. His fields of interest include power electronics, power quality, design of power filters, and distributed power generation.

Appendix A WSCC 9 Bus System Data

Generators:

Generator1: 600 MVA, 22 kV, 60 Hz,
 Generator2: 465 MVA, 22 kV, 60 Hz,
 Generator3: 310 MVA, 22 kV, 60 Hz.

Transformers:

Transformer1: 600 MVA, 22/400 kV, 60 Hz, $\Delta \cdot Y^{-1}$,
 Transformer2: 465 MVA, 22/400 kV, 60 Hz, $\Delta \cdot Y^{-1}$,
 Transformer3: 310 MVA, 22/400 kV, 60 Hz, $\Delta \cdot Y^{-1}$.

Loads:

Load A: 600MW+j100 MVAR,
 Load B: 200MW+j75 MVAR,
 Load C: 150MW+j75 MVAR.

Transmission Lines parameters:

Positive Sequence Parameters:

Resistance: $0.0329 \Omega \cdot \text{km}^{-1}$,
 Inductance: $0.964 \text{ mH} \cdot \text{km}^{-1}$,
 Capacitance: $11.441 \text{ nF} \cdot \text{km}^{-1}$.

Zero Sequence Parameters:

Resistance: $0.1587 \Omega \cdot \text{km}^{-1}$,
 Inductance: $3.114 \text{ mH} \cdot \text{km}^{-1}$,
 Capacitance: $3.394 \text{ nF} \cdot \text{km}^{-1}$.